Int. J. Anal. Appl. (2024), 22:148

International Journal of Analysis and Applications

Optimal Control Techniques in Managing Red Palm Weevil Infestations: A Mathematical Approach

Lamya Al-Maghamsi[1,*], Ymnah Alruwaily[2], Moustafa El-Shahed[3]

[1]*Department of Mathematics and Statistics, College of Science, University of Jeddah, P.O. Box: 80327 Jeddah 21589, Saudi Arabia*

[2]*Mathematics Department, College of Science, Jouf University, P.O. Box 2014, Sakaka 72388, Saudi Arabia ymnah@ju.edu.sa*

[3]*Department of Mathematics, College of Science, Qassim University, P.O. Box 6644, Buraydah 51452, Saudi Arabia*

[*]*Corresponding author:* lalmaghamsi@uj.edu.sa

Abstract. This article introduces a mathematical analysis of the red palm weevil (RPW) model that incorporates optimal control techniques. The investigation delves into the dynamics among date palm trees, the RPW, and tree micro-injection. The analysis assesses the impact of sex pheromone traps and tree trunk injections on the RPW population. Sufficient constraints are identified to provide both local stability and global stability analysis of equilibrium points. The paper uses Sotomayor's theorem as a guide to compute local bifurcations near equilibrium points. The study concludes that adopting control strategies shows to a substantial decline in the RPW population, ultimately resulting in extinction. Numerical simulations are employed to visually illustrate and support the theoretical findings.

1. Introduction

Red palm weevils *Rhynchophorus ferrugineus* are among the most destructive insects to palm trees worldwide. In the middle of the 1980s, it was found in Saudi Arabia in 1987 and the United Arab Emirates in 1986. It is well known that agricultural pests that attack date palms, particularly the RPW. Thus, date plantations lose a third of their productivity. The Gulf region has a favorable climate for growing palm trees, which makes it an ideal habitat for the red palm weevil. Countries in this region also have extensive palm plantations, including palm groves, which provide abundant food sources for the weevil [1–6].

Received: Jul. 10, 2024.

2020 *Mathematics Subject Classification.* 92B05, 37N25, 65L05.

Key words and phrases. red palm weevil; pheromone trap; mathematical model; optimization; bifurcation.

https://doi.org/10.28924/2291-8639-22-2024-148
ISSN: 2291-8639

One of the main reasons why it is difficult to control this pest is because of its biology. This is mainly because the life cycle of (RPW) the larval stage is within the palm. It creates tunnels in the palm stem, boring in various directions and at different depths. In red palm plantations worldwide, numerous methods have been implemented to control the red palm weevil (RPW). However, despite the widespread use of chemical insecticides as a control measure, studies have demonstrated that the application of these products inadvertently benefits the weevils by acting as artificial selection pressure [7]. One of the most crucial strategies for combating the RPW is the utilization of sex pheromone traps. These traps prevent insects from completing their life cycle and proliferating, as they contain insecticides that kill the trapped insects. This technique aims to collect and destroy entire insects [5, 8]. The researchers showed that using sex pheromone traps to disrupt mating is one of the most efficient techniques for controlling RPW [9–11]. In several places, tree micro-injection is used to eliminate some crop pests. To manage red palm weevils using traditional methods, there is a need to understand the technique of partial injection of trees, which has an effective role in eliminating the larvae, which are much more dangerous and destructive than their adults. By drilling several holes at specific angles into the palm stem, a chimerical compound will be injected into the stem. In the following case, after careful injection of the product into the palm stem, the product is moved upwards in order to target the site of the lesion. There is no movement of the pesticide down the tree roots which means it stays inside the tree. Leaves falling to the ground are quickly broken down by microorganisms. After treatment, trees or plants do not pose any threat to animals or workers in the immediate aftermath of treatment. Following [12], The compartmental model for red palm weevil exhibits symmetry, meaning that its differential equations are based on the idea that the rate of change of individuals within a specific compartment is equivalent to the influx of individuals minus the efflux of individuals. El-Shahed et.al. [13–15] proposed and analyzed a deterministic and stochastic model for RPW. The principal aim of this paper is to present and examine a mathematical model of the RPW with sex pheromone traps, taking into account the impact of optimal control on RPW dynamics. The focus is specifically on evaluating their effect on the RPW population. The manuscript is structured as below: In Section 2, we describe the RPW considered mathematical system and verify that the solutions of the RPW model are bounded. Section 3 examines the local and global stability of the RPW system. In Section 4, after determining the local bifurcation conditions, we investigate whether Hopf bifurcation eventuates at the coexistence equilibrium point. To confirm the obtained theoretical results, we illustrate some numerical simulations in the conclusion.

2. Mathematical model

In this part, based on the biological and ecological information presented, a considered model explaining the dynamics of the Red Palm Weevil population is established.

- Let $P(t)$ be the date palm tree population density. Without the presence of the RPW, we consider the growth rate r of the date palm grows, and k palm capacity.

- The larval stage and the adult stage are the two major stages of the RPW life cycle, respectively. The date palm tree will eventually die because the larval stage presents the greatest risk, as it destroys the palm tree's interior tissue in the trunk. Allow $L(t)$ to stand for the RPW larvae population density. The female and male RPWs ($F(t)$ and $M(t)$, respectively) make up the two compartments of the adult stage.
- Let θ_1 denote the tree Micro-injection of palm tree attacked by RPW larvae while θ represents the tree Micro-injection of palm tree attacked by adult RPW.
- From the larvae of the RPW, the adult weevils emerge at the rate α, female or male. Among the larvae that transform into an adult weevil, ϵ is the proportion that turns into a female, while $(1-\epsilon)$ is the complementary proportion that becomes male.
- Date palm consumption per RPW is represented as a Holling type-II response function $\frac{\beta P}{a+P}$. Date palm trees are preyed by RPWs at a rate of β. Whilst a determines the half-saturation point, in other words, half of maximum predation rate. Because not all date palm biomass is converted to RPW biomass, we assume that the conversion rate is $0 < e < 1$.
- In order to reduce RPW, we intend to restrict the use of female pheromone traps. First, the number of offspring is decreased by interfering with RPW mating in order to decrease the likelihood of fertilization. This is accomplished by setting up traps that release a female pheromone lure that males are drawn to. As a result, there are fewer males available to mate with nearby females, which lowers the likelihood of conception. Second, the RPW males that the traps attract are killed because the pesticides in the traps.
- We take into consideration the methods put out by Barclay et al. [16], Barclay et al. [17] and Anguelov et al. [18] to account for the impact of pheromone traps. Therefore, the strength of the trap is determined according to how many wild females will release an equivalent amount of pheromones. Following [18–22], the pheromone trap's effect is supposed to attract additional η females. This implies that $F+\eta$ is the total number of RPW females that attract RPW males in such a context. In particular, pheromone traps tend to attract males with probability $\left(\frac{\eta}{F+\eta}\right)$. Males attracted to pheromone traps have a mortality rate γ.

RPW with sex pheromone traps and tree micro-injections is stated in the below model.

$$\begin{aligned}
\frac{\mathrm{d}P}{\mathrm{d}t} &= rP(1-\frac{P}{k}) - \frac{\beta PL}{a+P} - \mu_1 P,\\
\frac{\mathrm{d}L}{\mathrm{d}t} &= \frac{e\beta PL}{a+P} - \alpha L - \mu_2 L - \theta_1 L,\\
\frac{\mathrm{d}F}{\mathrm{d}t} &= \epsilon\alpha L - \mu F - \theta F,\\
\frac{\mathrm{d}M}{\mathrm{d}t} &= (1-\epsilon)\alpha L - \frac{\gamma\eta M}{F+\eta} - \mu M - \theta M.
\end{aligned} \tag{2.1}$$

2.1. **Non-negativity and boundedness.** For the RPW system (2.1), it is important to include both positivity and boundedness because positivity indicates that the populations survive and boundedness can be seen as a natural restriction to growth as a result of limited resources.

Proposition 2.1. *Every solution of the RPW system* (2.1) *with positive initial conditions remains positive for all* $t > 0$

Proof. The right hand side of the system (2.1) is obviously continuously differentiable, and thus locally Lipschitz with respect to P, L, F, M. It follows that the RPW system (2.1) possesses a unique solution (P, L, F, M) for given positive initial values. From RPW system (2.1) with positive initial conditions, one obtains:

$$\begin{aligned} P(t) &= P(0)\exp\left\{\int_0^t \left[r(1-\frac{P(s)}{k}) - \frac{\beta L(s)}{a+P(s)} - \mu_1\right]ds\right\} \geq 0, \\ L(t) &= L(0)\exp\left\{\int_0^t \left[\frac{e\beta P(s)}{a+P(s)} - (\alpha + \mu_2 L + \theta_1)\right]ds\right\} \geq 0, \\ F(t) &= F(0)\exp\left\{\int_0^t \left[\epsilon\alpha\frac{L(s)}{F(s)} - \mu - \theta\right]ds\right\} \geq 0, \\ M(t) &= M(0)\exp\left\{\int_0^t \left[(1-\epsilon)\alpha\frac{L(s)}{M(s)} - \frac{\gamma\eta}{F(s)+\eta} - \mu - \theta\right]ds\right\} \geq 0. \end{aligned} \tag{2.2}$$

Thus the solution of RPW model (2.1) remains positive for all $t > 0$. □

Based on the first equation of the RPW system (2.1), one has $\frac{dP}{dt} \leq rP(1-\frac{P}{k}) - \mu_1 P$ and

$$\frac{dP}{dt} + (r-\mu_1)P \leq -\frac{r}{k}\left[P^2 - \frac{2k}{r}(r-\mu_1)P\right] \leq \frac{k}{r}(r-\mu_1).$$

By applying the comparison theorem of differential inequalities established by Birkhoff and Rota [23, 24], we derive $P(t) \leq P_1$, where $P_1 = \frac{k\rho}{r}$ and $\rho = r - \mu_1$. Consequently, the solutions of model (2.1) are bounded.

Theorem 2.1. *The solutions of Red Palm Weevil system* (2.1) *in* $\mathbb{R}^4_+$ *are uniformly bounded.*

Proof. Below [25, 26], consider, $\mathfrak{H}(t) = P(t) + L(t) + F(t) + M(t)$, then

$$\begin{aligned} \frac{d\mathfrak{H}(t)}{dt} &\leq rP\left(1-\frac{P}{k}\right) - \mu_1 P - \mu_2 L - \mu(F+M) - \frac{\gamma\eta M}{F+\eta} \\ &= \frac{-r}{k}\left(P - \frac{k}{2}\right)^2 + \frac{rk}{4} - \nu\mathfrak{H}(t), \end{aligned}$$

where, $\nu = min\{\mu, \mu_1, \mu_2\}$. Thus, $\frac{d\mathfrak{H}(t)}{dt} + \nu M \leq \frac{rk}{4}$. Applying the comparison theorem of differential inequality [23], one achieve $0 \leq \mathfrak{H}(t) \leq \frac{rk}{4\nu}$. The outcomes of Eq. (2.1) in $\mathbb{R}^4_+$ is uniformly bounded in

$$\Sigma = \left\{(P, L, F, M) \in \mathbb{R}^4_+ : \mathfrak{H}(t) \leq \frac{rk}{4\nu} + \varsigma, \text{ for any } \varsigma > 0\right\}.$$

□

Following [27], the offspring number R_0 can be obtained as follows

$$R_0 = \frac{e\beta k\rho}{\Psi(k\rho + ar)},$$

where $\Psi = \alpha + \theta_1 + \mu_2$, $\Omega = \theta + \mu$.

3. Equilibria and stability

There are three equilibrium points of the RPW model (2.1):

(1) E_0, defined as $(0,0,0,0)$.
(2) The free RPW equilibrium point $E_1 = \left(\frac{k\rho}{r}, 0, 0, 0\right)$. E_1 exists if $r > \mu_1$
(3) The coexistence equilibrium point $E_2 = (P_2, L_2, F_2, M_2)$, where

$$P_2 = \frac{a\Psi}{e\beta - \Psi},\ L_2 = \frac{a + P_2}{\beta}\left[\rho - \frac{rP_2}{k}\right],\ F_2 = \frac{\epsilon\alpha L_2}{\Omega},\ \ M_2 = \frac{(1-\epsilon)\alpha L_2(\eta + F_2)}{\gamma\eta + \Omega(\eta + F_2)}.$$

When $R_0 > 1$, E_2 exists positively as a coexistence equilibrium point. At the equilibrium points, there is symmetry since the population's rate of change is zero.

We will discuss the locally asymptotically stable ($\mathcal{LAS}$) equilibrium points and the globally asymptotically stable ($\mathcal{GAS}$) equilibrium points of RPW system (2.1). Following [28–30], the Jacobian matrix of RPW system (2.1)is defined in general form as:

$$J = \begin{pmatrix} r - \frac{2P}{k}r - \frac{a\beta L}{(a+P)^2} - \mu_1 & \frac{-\beta P}{a+P} & 0 & 0 \\ \frac{ea\beta L}{(a+P)^2} & \frac{e\beta P}{a+P} - \Psi & 0 & 0 \\ 0 & \epsilon\alpha & -\Omega & 0 \\ 0 & (1-\epsilon)\alpha & \frac{\gamma\eta M}{(F+\eta)^2} & -\frac{\gamma\eta}{F+\eta} - \Omega \end{pmatrix} \tag{3.1}$$

The following two theorems are presented to examine the stability of RPW extinction equilibrium point $E_0 = (0,0,0,0)$,

Theorem 3.1. *If $r < \mu_1$, then E_0 is $\mathcal{LAS}$.*

Proof. The Jacobian matrix at E_0, takes the form:

$$J(E_0) = \begin{pmatrix} r - \mu_1 & 0 & 0 & 0 \\ 0 & -\Psi & 0 & 0 \\ 0 & \epsilon\,\alpha & -\Omega & 0 \\ 0 & (1-\epsilon)\alpha & 0 & -\Omega - \gamma \end{pmatrix}. \tag{3.2}$$

The eigenvalues of $J(E_0)$ are $\lambda_1 = r - \mu_1$, $\lambda_2 = -\Omega - \gamma$, $\lambda_3 = -\Psi$ and $\lambda_4 = -\Omega$. When $r < \mu_1$, the eigenvalues of $J(E_0)$ is a negative part in E_0 . By Routh-Hurwitz assumption E_0 is $\mathcal{LAS}$ provided that $r < \mu_1$. □

Theorem 3.2. *If $r < \mu_1$ and $\omega < \theta + \mu$, then E_0 is $\mathcal{GAS}$.*

Proof. By using Lyapunov function $\Psi_1(t) = P(t) + L(t) + F(t) + M(t)$, which is $\frac{d\Psi_1}{dt}$ along the result of RPW system (2.1) gives:

$$\begin{aligned} \frac{d\Psi_1}{dt} &\leq rP\left(1 - \frac{P}{k}\right) - \mu_1 P - \mu_2 L - \theta_1 L \\ &\leq (r - \mu_1)P + (\omega - \theta - \mu)F. \end{aligned}$$

Taking $r < \mu_1$, one gets $\frac{d\Psi_1}{dt} \leq 0$, therefore E_0 is $\mathcal{GAS}$. □

Here we examine the stability of $E_1 = (P_1, 0, 0, 0)$, which is the free RPW equilibrium point.

Theorem 3.3. *If $R_0 < 1$, $R_1 < 1$ and $\rho > 0$, then E_1 is $\mathcal{LAS}$.*

Proof. At E_1, the Jacobian matrix has the following form:

$$J(E_1) = \begin{pmatrix} -\rho & \frac{-\beta k\rho}{k\rho+ar} & 0 & 0 \\ 0 & \frac{e\beta k\rho}{k\rho+ar} - \Psi & 0 & 0 \\ 0 & \epsilon\alpha & -\Omega & 0 \\ 0 & (1-\epsilon)\alpha & 0 & -\gamma-\Omega \end{pmatrix},$$

The eigenvalues of $J(E_1)$ are $\lambda_1 = -\rho$, $\lambda_2 = -\Omega - \gamma$ and the other tow roots are determined by $\lambda^2 + (\Psi + \Omega)(1 - R_1)\lambda + \Psi\Omega(1 - R_0) = 0$, where $R_1 = \frac{e\beta k\rho}{(k\rho+ar)(\Psi+\Omega)}$. It can be observed that if $R_0 < 1, R_1 < 1$ and $\rho > 0$, then E_1 is $\mathcal{LAS}$. □

Theorem 3.4. *If $e_1\beta P_1 < a(\mu_2 + \theta_1)$, then E_1 is $\mathcal{GAS}$.*

Proof. Assume the below positive given Lyapunov function:

$$\Psi_2(t) = e\left(P - P_1 - P_1 \ln(\frac{P}{P_1})\right) + L(t) + F(t) + M(t),$$

calculating $\frac{d\Psi_2}{dt}$, we obtain,

$$\begin{aligned} \frac{d\Psi_2}{dt} &\leq e(P - P_1)\left[r\left(1 - \frac{P}{k}\right) - \mu_1 - \frac{\beta L}{a+P}\right] + \frac{e\beta PL}{a+P} - (\mu_2 + \theta_1)L \\ &\leq \frac{-er}{k}(P - P_1)^2 + \left(\frac{e\beta P_1}{a+P} - (\mu_2 + \theta_1)\right)L. \end{aligned}$$

Choosing $e\beta P_1 < (a + P^2)(\mu_2 + \theta_1)$, one obtains $\frac{d\Psi_2}{dt} \leq 0$, therefore, free RPW equilibrium point E_1 is $\mathcal{GAS}$.

□

As follows, we investigate the stability of $E_2 = (P_2, L_2, F_2, M_2)$.

Theorem 3.5. *If $\frac{\beta L_2}{(a+P_2)^2} > \frac{rP_2}{k}$ and $\frac{e\beta P_2}{a+P_2} > \Psi$, then E_2 is $\mathcal{LAS}$*

Proof. At E_2, the Jacobian matrix of RPW Eq. (2.1) given below

$$J(E_2) = \begin{pmatrix} \frac{\beta L_2}{(a+P_2)^2} - \frac{rP_2}{k} & \frac{-\beta P}{a+P} & 0 & 0 \\ \frac{ea\beta L_2}{(a+P_2)^2} & \frac{e\beta P_2}{a+P_2} - \Psi & 0 & 0 \\ 0 & \epsilon\alpha & -\Omega & 0 \\ 0 & (1-\epsilon)\alpha & \frac{\gamma\eta M_2}{(F_2+\eta)^2} & -\frac{\gamma\eta}{F_2+\eta} - \Omega \end{pmatrix} \tag{3.3}$$

The first eigenvalue of $J(E_2)$ is $\lambda_1 = -\frac{\gamma\eta}{F_2+\eta} - \Omega$. The other roots are determined by

$$\lambda^3 + \left(A_1 + \frac{\epsilon\alpha\omega}{\Omega} + \Omega\right)\lambda^2 + (A_1\omega + A_2A_3)\,\lambda + A_2A_3\Omega = 0, \tag{3.4}$$

where

$$A_1 = \frac{\beta L_2}{(a+P_2)^2} - \frac{rP_2}{k},\ A_2 = \frac{ea\beta L_2}{(a+P_2)^2},\ \ A_3 = \frac{e\beta P_2}{a+P_2} - \Psi.$$

When $A_1 > 0$ and $A_3 > 0$, then all the eigenvalues of $J(E_2)$ near the E_2 which satisfies the Routh–Hurwitz points E_2 is $\mathcal{LAS}$. □

4. Bifurcation analysis

Using Sotomayor's theorem [31], this section discusses the local bifurcations of the RPW model(2.1) near the equilibrium points. Vector representation of the RPW model (1) is as $\frac{dX}{dt} = G(X)$, such that $X = P, L, F, M)^T$, $G = (\xi_1, \xi_2, \xi_3, \xi_4)^T$ with $\mathfrak{f}_i, i = 1...4$ of the RPW Eq. (2.1), right side.

Theorem 4.1. *Transcritical bifurcation of the RPW system (1) with respect to the bifurcation parameter r occurs around E_0 if $r = \mu_1$.*

Proof. We define the eigenvector V_1 corresponding to the eigenvalue $\lambda = 0$ of $J(E_0)$ as $V_1 = (\nu_1, \nu_2, \nu_3, \nu_4)^{\mathrm{T}}$, hence $J(E_0)V_1 = 0$, gives $V_1 = (\nu_1, 0, 0, 0)^{\mathrm{T}}$, ν_1 is a real number. By same procedure, Such that the eigenvector V_2, the eigenvalue $\lambda = 0$ of $J(E_0)^{\mathrm{T}}$ as $V_2 = (\tau_1, \tau_2, \tau_3, \tau_4)^{\mathrm{T}}$, Where, $J(E_0)^{\mathrm{T}}V_2 = 0$ provies $V_2 = (\tau_1, 0, 0, 0)$ where, real number τ_1. Suppose, $\frac{\partial G}{\partial r} = G_r(X, r) = (P(1 - \frac{P}{k}), 0, 0, 0)^{\mathrm{T}}$, therefore, $V_2^{\mathrm{T}}\, G_r(E_0, r^*) = 0$. Due to Sotomayor's technique, the RPW model (1) does not have saddle-node bifurcations near E_0 at $r^* = \mu_1$.

Now,

$$DG_r(E_0, r^*) = \begin{pmatrix} 1 & 0 & 0 & 0 \\ 0 & 0 & 0 & 0 \\ 0 & 0 & 0 & 0 \\ 0 & 0 & 0 & 0 \end{pmatrix},$$

then $V_2^{\mathrm{T}} DG_r(E_0, r^*)V_1 = \nu_1\tau_1 \neq 0$. Consequently

$$V_2^{\mathrm{T}} D^2 G(X, r)(V_1, V_1) = -\frac{2r\tau_1\zeta_1^2}{k} \neq 0$$

A transcritical bifurcation occurs at $r^* = \mu_1$ for the RPW system (1) based on Sotomayor's theorem. □

Theorem 4.2. *Transcritical bifurcation of the RPW system (1) by employing bifurcation parameter θ_1 occurs around around $E_1 = (P_1, 0, 0, 0)$ if $R_0 = 1$.*

Proof. By the help of Jacobian matrix of the RPW the Eq. (2.1) at E_1 with $\theta_1 = \theta_1^* = \frac{e\beta k\rho}{(k\rho + ar)} - \alpha - \mu_2$ has zero eigenvalue takes the form

$$J(E_1) = \begin{pmatrix} -\rho & \frac{-\beta k\rho}{k\rho + ar} & 0 & 0 \\ 0 & 0 & 0 & 0 \\ 0 & \epsilon\alpha & -\Omega & 0 \\ 0 & (1-\epsilon)\alpha & 0 & -\gamma - \Omega \end{pmatrix},$$

The eigenvector corresponding to $J(E_1)V_3 = 0$, given below,

$$V_3 = \begin{pmatrix} \frac{-\beta P_1^2(\Omega+\gamma)k}{(a+P_1^2)(1-\epsilon)\alpha(2rP_1+k(\mu-r))}\nu_2 \\ \frac{(\Omega+\gamma)}{(1-\epsilon)\alpha}\nu_2 \\ \frac{(\Omega+\gamma)\epsilon}{(1-\epsilon)\Omega}\nu_2 \\ \nu_2 \end{pmatrix},$$

where ν_2 is any non zero real number. By the same way, the eigenvector corresponding to $J(E_1)^{\mathrm{T}}V_4 = 0$ is $V_4 = (0, \tau_2, 0, 0)^{\mathrm{T}}$ where τ_2 is a non-zero real number. Let, $\frac{\partial G}{\partial \theta_1} = G_{\theta_1}(X, \theta_1) = (0, -L, 0, 0)^{\mathrm{T}}$, thus, $V_4^{\mathrm{T}}\, G_{\theta_1}(E_1, \theta_1^*) = 0$. Due to Sotomayor's local bifurcation theorem, the RPW model (1) does not have saddle-node bifurcations near E_1 at $\theta_1^* == \frac{e\beta k\rho}{(k\rho+ar)} - \alpha - \mu_2$.
Now,

$$DG_{\theta_1}(E_1, {\theta_1}^*) = \begin{pmatrix} 0 & 0 & 0 & 0 \\ 0 & -1 & 0 & 0 \\ 0 & 0 & 0 & 0 \\ 0 & 0 & 0 & 0 \end{pmatrix},$$

then $V_4^{\mathrm{T}} DG_{\theta_1}(E_1, {\theta_1}^*)V_3 = \frac{-(\Omega+\gamma)}{(1-\epsilon)\alpha}\nu_3\tau_3$. As a result

$$V_4^{\mathrm{T}} D^2G(X, \theta_1)(V_3, V_3) = \frac{4a\beta e\tau_2}{(a+P_1)^2}\zeta_1\zeta_2 \neq 0$$

Based on Sotomayor's theorem, the RPW Eq. (1) satisfies all the criteria of transcritical bifurcation at $\theta_1^* = \frac{e\beta k\rho}{(k\rho+ar)} - \alpha - \mu_2$. □

5. Optimal control of RPW

In order to reduce the number of red palm weevils over time t, control procedures are proposed in this section using the principles of optimal control theory. Two constrained controls, $u_1(t)$ and $u_2(t)$, are thus introduced to the system (2.1). Therefore the red palm weevil model with two controls takes the form

$$\begin{aligned} \frac{\mathrm{d}P}{\mathrm{d}t} &= rP(1-\frac{P}{k}) - \frac{\beta PL}{a+P} - \mu_1 P \\ \frac{\mathrm{d}L}{\mathrm{d}t} &= \frac{e\beta PL}{a+P} - \alpha L - \mu_2 L - \theta_1 L - u_1 L, \\ \frac{\mathrm{d}F}{\mathrm{d}t} &= \epsilon\alpha L - \mu F - \theta F - u_2 F, \\ \frac{\mathrm{d}M}{\mathrm{d}t} &= (1-\epsilon)\alpha L - \frac{\gamma\eta M}{F+\eta} - \mu M - \theta M - u_2 M, \end{aligned} \tag{5.1}$$

where $P(0) = P_0$, $L(0) = L_0$, $F(0) = F_0$, $M(0) = M_0$. The objective is to find a pattern to minimize the number of Larvae and adult RPW spreading the infection using the following functional

$$J(u_1(t), u_2(t)) = \min \int_0^{\mathrm{T}} \left[L + F + M + c_1u_1^2 + c_2u_2^2\right] dt,$$

where c_1 and c_2 are positive weight constants. One can seek a pair (u_1^*, u_2^*) of the optimal control problem such that:

$$J(u_1^*(t), u_2^*(t)) = \min\{J(u_1(t), u_2(t))|(u_1, u_2) \in U_0\},$$

where $U_0 = \left\{(u_1, u_2) : 0 \leq u_j \leq 1, u_j \text{ is measurable}, t \in [t, t_e], j = 1, 2\right\}$. Utilizing the Pontryagin's maximum principle [32–36], one can determine the condition for the control of of the RPW system (5.1) as follows.

$$\begin{aligned} H =& L + F + M + c_1u_1^2 + c_2u_2^2 + \xi_1\left(rP(1-\frac{P}{k}) - \frac{\beta PL}{a+P} - \mu_1 P\right) \\ &+ \xi_2\left(\frac{e\beta PL}{a+P} - \alpha L - \mu_2 L - \theta_1 L - u_1 L\right) + \xi_3\left(\epsilon\alpha L - \mu F - \theta F - u_2 F\right) \\ &+ \xi_4\left((1-\epsilon)\alpha L - \frac{\gamma\eta M}{F+\eta} - \mu M - \theta M - u_2 M\right), \end{aligned}$$

where $\xi_j(t), j = 1, 2, 3, 4$ are the co-state variables to be determined. According to Pontryagin's maximum principle, one can get the following adjoint equations.

$$\begin{aligned} \frac{\mathrm{d}\xi_1}{\mathrm{d}t} &= -\frac{\partial H}{\partial P} = -\xi_1\left[r - \frac{2rP}{k} - \frac{a\beta L}{(a+P)^2} - \mu_1\right] - \xi_2\left(\frac{e\beta aL}{(a+P)^2}\right) \\ \frac{\mathrm{d}\xi_2}{\mathrm{d}t} &= -\frac{\partial H}{\partial L} = -1 + \xi_1\frac{\beta P}{(a+P)} - \xi_2\left(\frac{e\beta P}{a+P} - \Psi - u_1\right) - \xi_3\epsilon\alpha - \xi_4(1-\epsilon)\alpha, \\ \frac{\mathrm{d}\xi_3}{\mathrm{d}t} &= -\frac{\partial H}{\partial F} = -1 + \xi_3(\Omega + u_2) - \xi_4\left(\frac{\gamma\eta M}{(F+\eta)^2}\right), \\ \frac{\mathrm{d}\xi_4}{\mathrm{d}t} &= -\frac{\partial H}{\partial M} = -1 + \xi_4\left(\frac{\gamma\eta}{F+\eta} + \Omega + u_2\right), \end{aligned} \tag{5.2}$$

with the boundary conditions $\xi_j(t_e) = 0,\ j = 1, 2, 3, 4$ The optimality criteria for the system 5.2 deduce to

$$\begin{aligned} \frac{\partial H}{\partial u_1} &= 2c_1u_1 - \xi_2 L \\ \frac{\partial H}{\partial u_2} &= 2c_2u_2 - \xi_3 F - \xi_4 M, \end{aligned}$$

Using $\frac{\partial H}{\partial u_1} = 0$ and $\frac{\partial H}{\partial u_2} = 0$ at $u_1 = u_1^*$ and $u_2 = u_2^*$, yields

$$u_1^* = \frac{\xi_2 L}{2c_1}, \qquad u_2^* = \frac{\xi_3 F + \xi_4 M}{2c_2}$$

Consequently

$$u_1^*(t) = \begin{cases} 0 & \text{if } u_1 \leq 0, \\ \frac{\xi_2 L}{2c_1} & \text{if } 0 < u_1^* < 1, \\ 1 & \text{if } u_1^* > 1 \end{cases}$$

$$u_2^*(t) = \begin{cases} 0 & \text{if } u_2 \leq 0, \\ \frac{\xi_3 F + \xi_4 M}{2c_2} & \text{if } 0 < u_2^* < 1, \\ 1 & \text{if } u_2^* > 1 \end{cases}$$

which, can be rewritten in the following compact form

$$u_1^*(t) = \min\left\{\max\left\{0, \frac{\xi_2 L}{2c_1}\right\}, 1\right\} \quad \text{and} \quad u_2^*(t) = \min\left\{\max\left\{0, \frac{\xi_3 F + \xi_4 M}{2c_2}\right\}, 1\right\}. \tag{5.3}$$

The red palm weevil systems 5.1,5.2, and 5.3, by numerically solving to obtain the best controls.

6. Numerical simulations

To illustrate the previously theoretical findings, numerical simulations of the Red Palm Weevil system (2.1) are taken out in this section. Date palms and red palm weevils will be numerically studied by using the below parameters [13,14]: $r = 0.5$, $k = 3$, $\beta = 0.9$, $\mu_1 = 0.01$, $\mu_2 = 0.002$, $\mu = 0.001$, $\alpha = 0.1$, $a = 3$, $\theta = 0.03$, $e = 0.2$, $\gamma = 0.2$, $\epsilon = 0.6$, $\eta = 0.02$.

As demonstrated in Fig. 1, the parameter η has a significant impact on the Red Palm Weevil male population density. The population density of male Red Palm Weevils declines with increasing η, as seen in Fig. 1. We conclude that the parameters η can regulate the dynamics of the considered model. Similarly, as can be seen in Fig. 2 the Tree Micro-injection parameter θ significantly affects the Red Palm Weevil male population density. According to Fig. 2, the male Red Palm Weevil population density decreases as θ increases. From this, we infer that the Red Palm Weevil's dynamics can be controlled by Micro-injection parameter θ. In Fig. 3 and theorem (4.1), we display the bifurcation graphs concerning r as a bifurcation parameter to illustrate the impact of the Palm tree's intrinsic growth rate, r. It can be demonstrated that a transcritical bifurcation occurs at $r = 0.01$ if the growth rate r is increased while maintaining the values of all other parameters. We change the value of β while holding the values of all other parameters to better understand how the red palm weevil system model 2.1 changes dynamically in reaction to shifts in the amount of predation between palm tree and weevil. Fig. 4 and theorem (4.2) both demonstrate that a transcritical bifurcation occurs at $\beta = 0.7476035115$. To explain the effect of carrying capacity k of the palm tree, We construct the bifurcation diagram concerning k as a bifurcation parameter, as indicated in Fig. 5 and theorem 4.2, a transcritical bifurcation occurs at $k = 3.3843$. Moreover, it can be seen that the Red Palm Weevil free equilibrium point$E1 = (P_1, 0, 0, 0)$ is asymptotically locally stable when $3.3843 < k < 9.2114$. According to Fig. 5 and the theorem3.5, a Hopf bifurcation happens at $k = 9.211$. This is visible from the last three figures, starting with Fig. 6 when $k = 1.5$, but changing k to 7 changed the solution behavior to Fig. 7, and Fig. 8 depicts the Hopf bifurcation meaning when we adjusted k to 17. Based on Figures 10, 11 and 12, it can be observed that the adoption of control strategies leads to a significant decline in the population of red palm weevil larvae, adult females, and males, eventually leading to their extinction. Finally, Fig 13, represents the control variables $u_1(t)$ and $u_2(t)$ as a function of time.

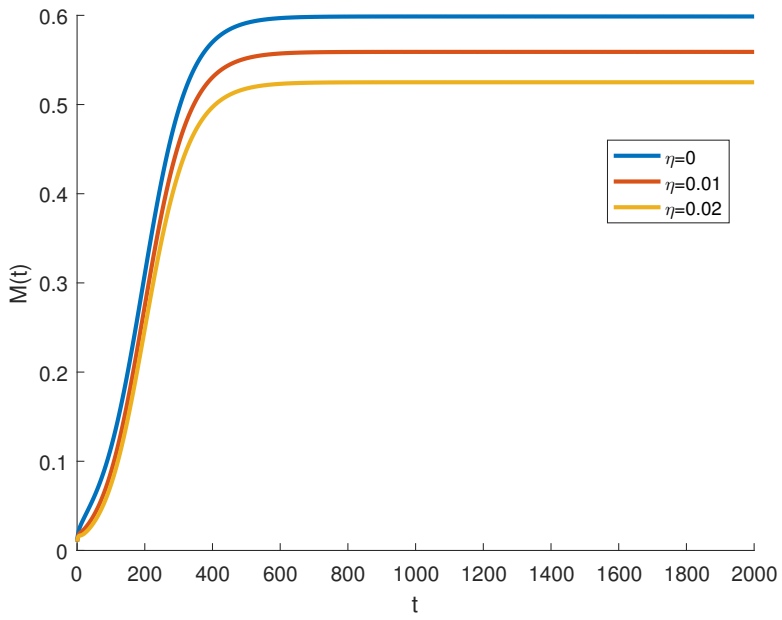

FIGURE 1. Dynamical illustration of the model (2.1) with $\eta = 0,\ 0.01,\ 0.02$

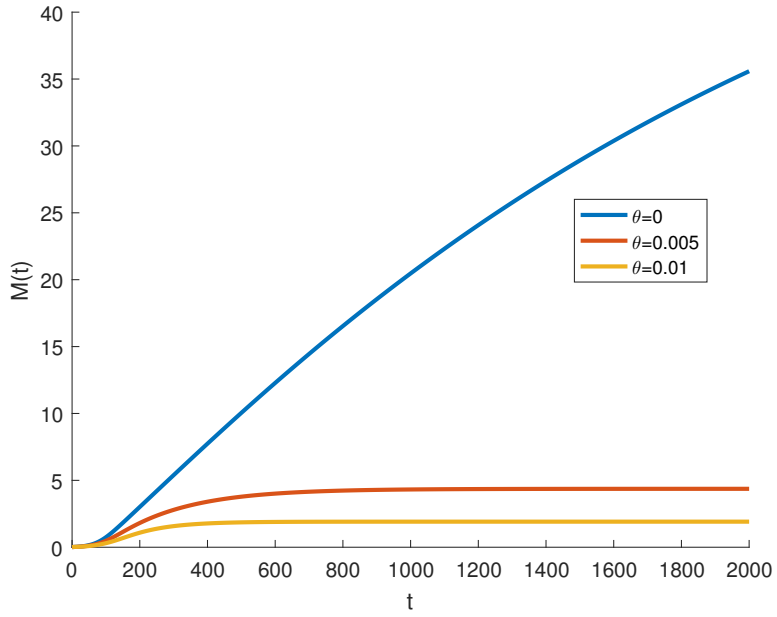

FIGURE 2. Dynamical illustration of the model (2.1) with $\theta = 0,\ 0.005,\ 0.01$

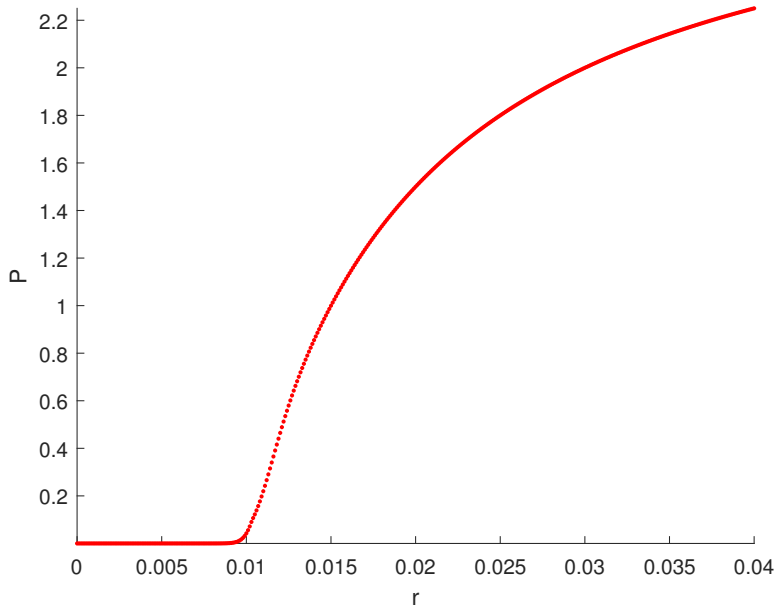

FIGURE 3. Bifurcation demonstration of Red Palm Weevil system (2.1) to $r, 0 \leq r \leq 0.04$ values

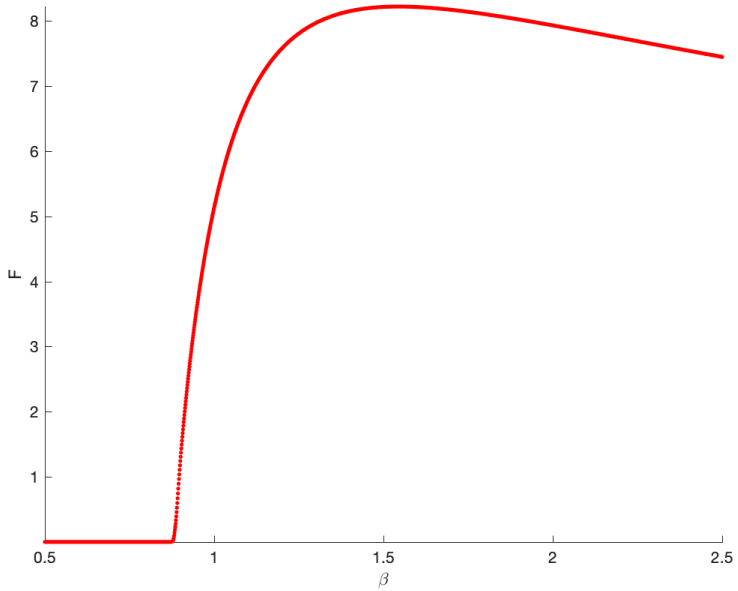

FIGURE 4. Bifurcation graph of Red Palm Weevil model (2.1) with respect to β

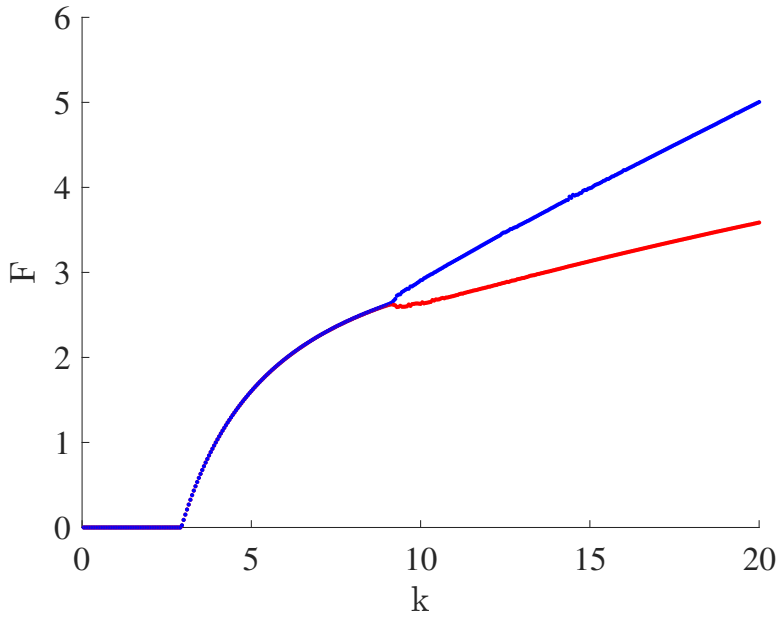

FIGURE 5. Bifurcation graph of Red Palm Weevil model (2.1) with respect to k

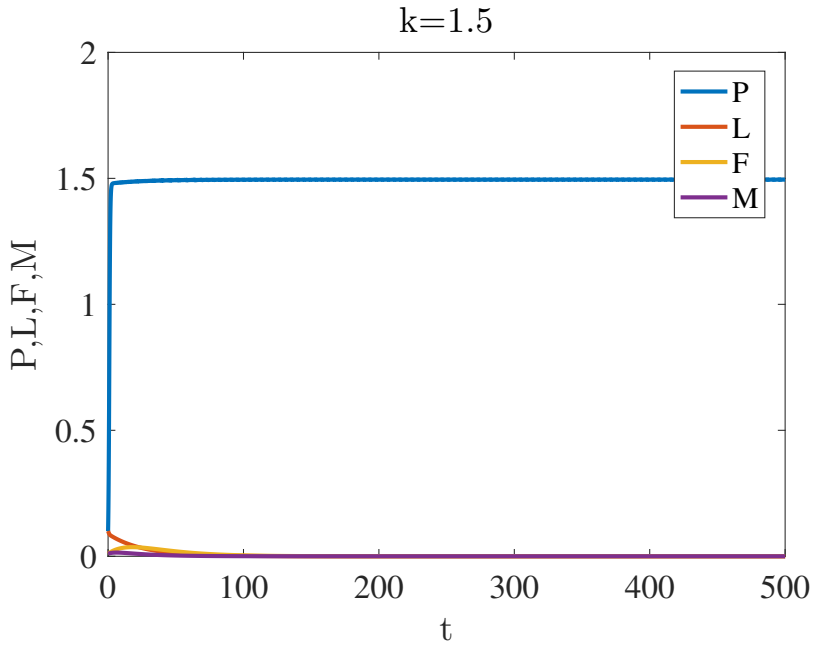

FIGURE 6. Dynamical illustration of the model (2.1) with $k = 1.5$

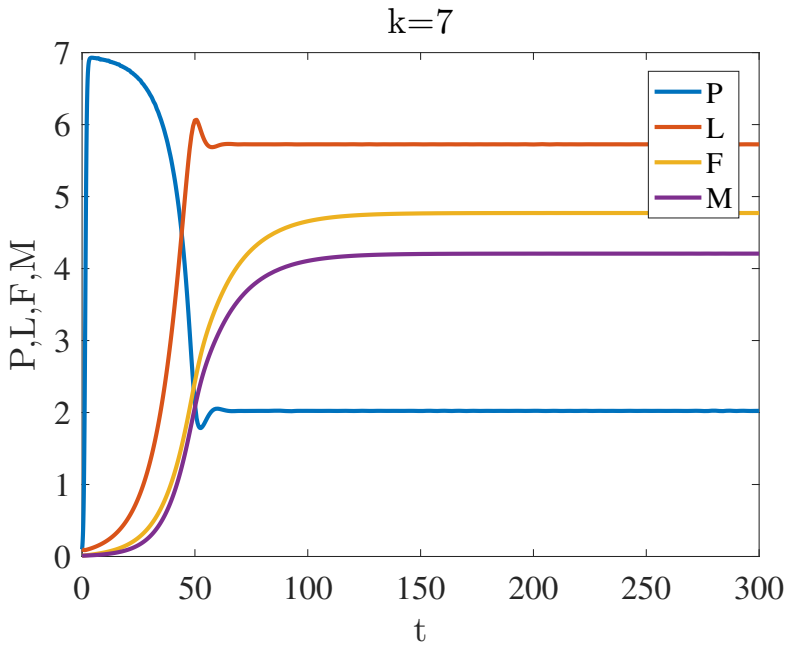

FIGURE 7. Dynamical illustration of the system (2.1) with $k = 7$

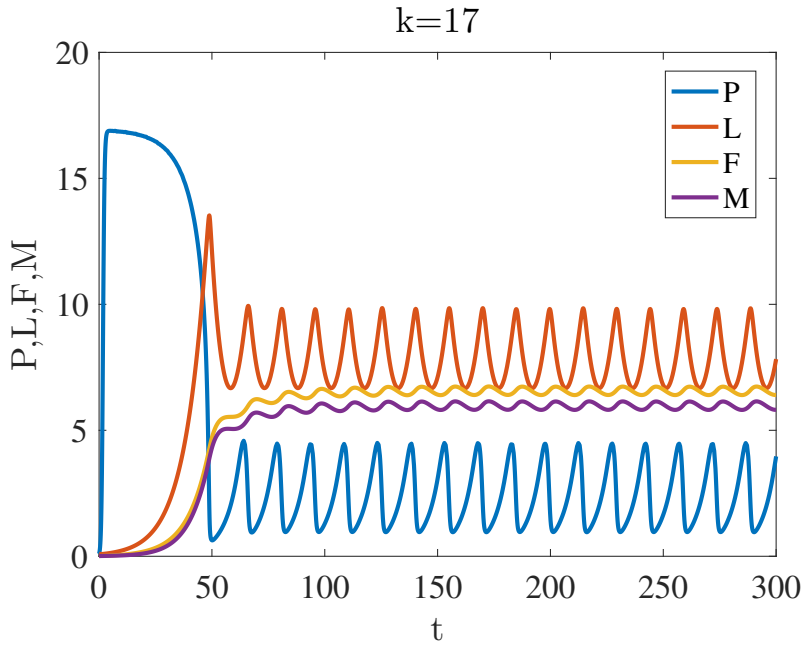

FIGURE 8. Dynamical illustration of the model (2.1) with $k = 17$

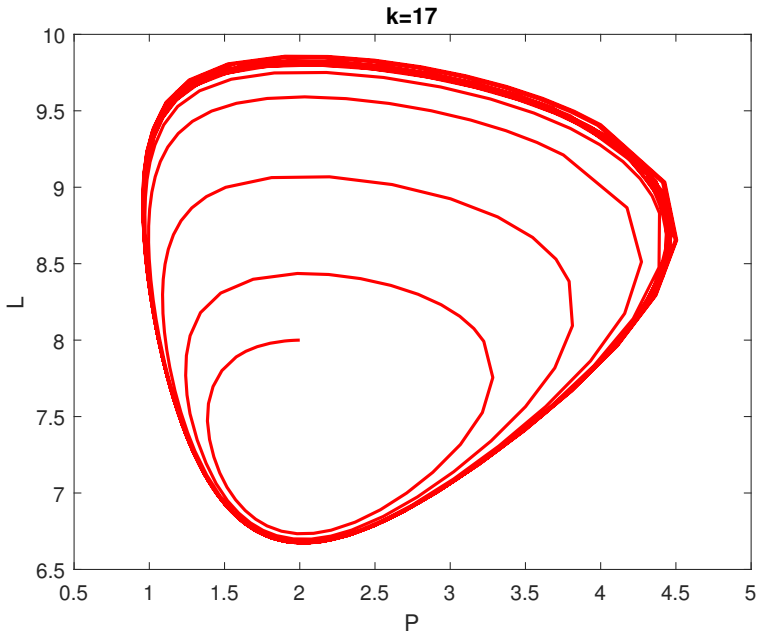

FIGURE 9. Phase portrait of model(2.1) with $k = 17$

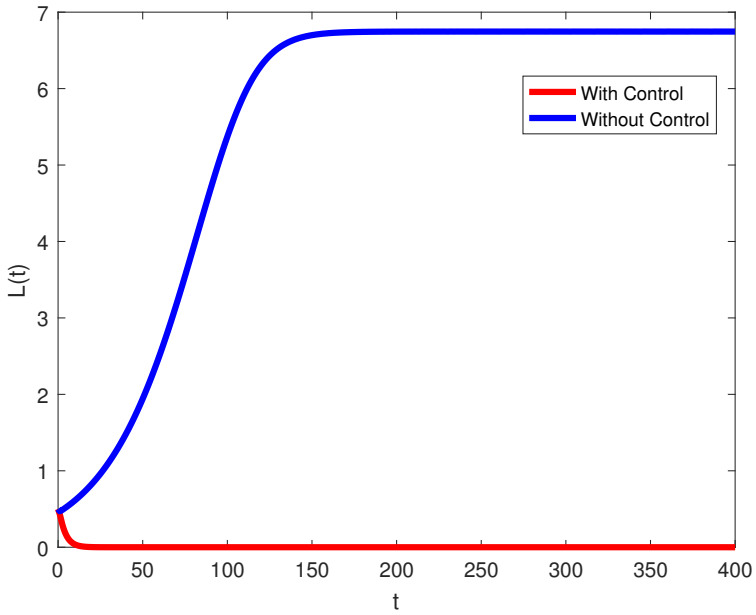

FIGURE 10. The effect of optimal control on the Larvae population $L(t)$

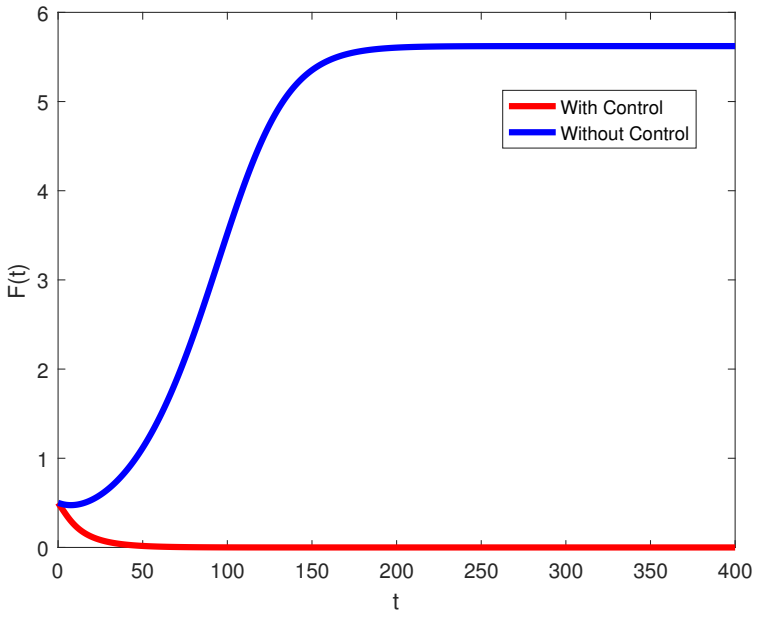

FIGURE 11. The effect of optimal control on the Larvae population $F(t)$

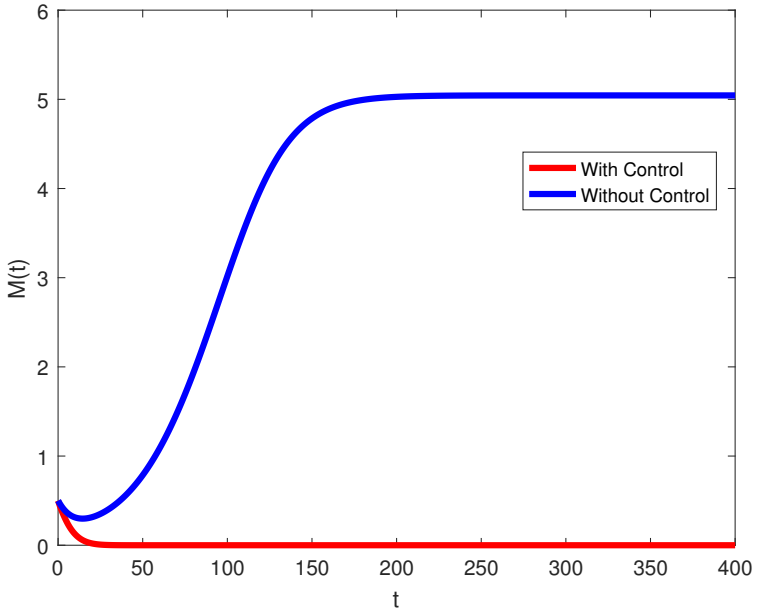

FIGURE 12. The effect of optimal control on the Larvae population $M(t)$

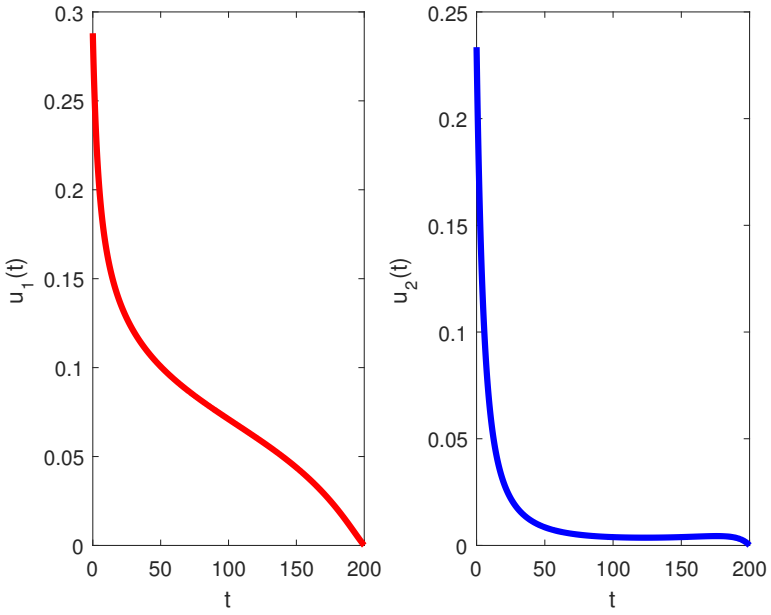

FIGURE 13. The graph represents the control variables $u_1(t)$ and $u_2(t)$

7. Discussion and Conclusion

This study incorporates a mathematical model for the Red Palm Weevil utilizing sex pheromone traps and tree micro-injections. We have studied how sex pheromone traps influence the spread of the red palm weevil. Studies have been made into how the red palm weevil and date palm tree interacted. To guarantee local $\mathcal{LAS}$ and global $\mathcal{GAS}$ stability equilibrium points, we found some conditions. The equilibrium, E_1, has been demonstrated to be locally asymptotically stable for $R_0 < 1$. We can infer from theorem (4.2) that the RPW model has a transcritical bifurcation for $R_0 = 1$. Theorem (3.3) shows a Hopf bifurcation in the Red Palm Weevil model when carrying capacity k controls the bifurcation. We observed that sex pheromone traps can control Red Palm Weevil. With the aid of Sotomayor's theorem, the occurrence of local bifurcation close to the equilibrium point is calculated. Without numerical examples of the analytical conclusions, analytical studies are never performed. Thus, all analytical conclusions are supported by data and figures. Numerical simulations are presented here that demonstrate the dynamical behavior of the system and agree well with the analytical results. We have found that Red Palm Weevil male population density is regulated by the sex pheromone trap parameter η. However, we focused on only a theoretical analysis of such scenarios, despite providing a realistic mathematical model of pheromone traps and tree injections for controlling Red Palm Weevil. Without the use of chemical pesticide resistance to the insect, our theoretical analysis can identify the primary mechanisms involved in Red Palm Weevil control utilizing pheromone traps. It would be highly advantageous to develop a mathematical model that incorporates pheromone traps, tree Micro-injection, pesticides, and mechanical resistance to control the Red Palm Weevil. As a result of the numerical simulation of

the red palm weevil, it can be concluded that the optimal control policy, through stem injections and chemical pesticides, has a significant effect in making the red palm weevil system free from pests and maintaining a stable nature in the remaining period. The model examined here could be improved in subsequent work to enhance the mathematical system of this article to describe and explain the effect of pesticides in RPW control in the presence of pheromone traps and tree Micro-injection. Checking whether the mechanisms identified by the model behave similarly in the real world may require further empirical or field research in this area. In the present work, we assumed that temperature, environmental influence, and all other conditions were homogeneous, but this assumption is not so. For the following studies, one can consider the heterogeneous red palm weevil system.

Funding: This work was funded by the University of Jeddah, Jeddah, Saudi Arabia, under grant No. (UJ-23-DR-7). Therefore, the authors thank the University of Jeddah for its technical and financial support.

Authors' contributions: All authors contributed equally to the writing of this paper. All authors read and approved the final manuscript.

Conflicts of Interest: The authors declare that there are no conflicts of interest regarding the publication of this paper.

References

[1] L.I. El-Juhany, Degradation of Date Palm Trees and Date Production in Arab Countries: Causes and Potential Rehabilitation, Aust. J. Basic Appl. Sci. 4 (2010), 3998–4010.

[2] J.M. Al-Khayri, Date Palm Phoenix dactylifera L. Micropropagation, in: S.M. Jain, H. Häggman (Eds.), Protocols for Micropropagation of Woody Trees and Fruits, Springer, Dordrecht, 2007: pp. 509–526. https://doi.org/10.1007/978-1-4020-6352-7_46.

[3] A. Levi-Zada, D. Fefer, L. Anshelevitch, A. Litovsky, M. Bengtsson, G. Gindin, V. Soroker, Identification of the Sex Pheromone of the Lesser Date Moth, Batrachedra Amydraula, Using Sequential SPME Auto-Sampling, Tetrahedron Lett. 52 (2011), 4550–4553. https://doi.org/10.1016/j.tetlet.2011.06.091.

[4] M. A. Al-Deeb, H. A. Al-Dhaheri, Use of a Pheromone-Baited Trap to Monitor the Population of the Lesser Date Moth Batrachedra Amydraula (Lepidoptera: Batrachedridae) in the UAE, J. Entomol. Zool. Stud. 5 (2017), 2572–2575.

[5] M.S. Hoddle, A.H. Al-Abbad, H.A.F. El-Shafie, J.R. Faleiro, A.A. Sallam, C.D. Hoddle, Assessing the Impact of Areawide Pheromone Trapping, Pesticide Applications, and Eradication of Infested Date Palms for Rhynchophorus Ferrugineus (Coleoptera: Curculionidae) Management in Al Ghowaybah, Saudi Arabia, Crop Protect. 53 (2013), 152–160. https://doi.org/10.1016/j.cropro.2013.07.010.

[6] I. Milosavljević, H.A.F. El-Shafie, J.R. Faleiro, C.D. Hoddle, M. Lewis, M.S. Hoddle, Palmageddon: The Wasting of Ornamental Palms by Invasive Palm Weevils, Rhynchophorus spp., J. Pest. Sci. 92 (2018), 143–156. https://doi.org/10.1007/s10340-018-1044-3.

[7] M. Ponce-Méndez, M.A. García-Martínez, R. Serna-Lagunes, R. Lasa-Covarrubias, E. Presa-Parra, J. Murguía-González, C. Llarena-Hernández, Local Agricultural Management Filters Morphological Traits of the South American Palm Weevil (Rhynchophorus palmarum L.; Coleoptera: Curculionidae) in Ornamental Palm Plantations, Agronomy. 12 (2022), 2371. https://doi.org/10.3390/agronomy12102371.

[8] R.T. Carde, Using Pheromones to Disrupt Mating of Moth Pests, In: Perspectives in Ecological Theory and Integrated Pest Management, Cambridge University Press, Cambridge, pp. 122–169, 2007.

[9] W. Wakil, J. Romeno Faleiro, T.A. Miller, eds., Sustainable Pest Management in Date Palm: Current Status and Emerging Challenges, Springer, Cham, 2015. https://doi.org/10.1007/978-3-319-24397-9.

[10] P. Witzgall, P. Kirsch, A. Cork, Sex Pheromones and Their Impact on Pest Management, J. Chem. Ecol. 36 (2010), 80–100. https://doi.org/10.1007/s10886-009-9737-y.

[11] H.J. Barclay, G.J.R. Judd, Models for Mating Disruption by Means of Pheromone for Insect Pest Control, Popul. Ecol. 37 (1995), 239–247. https://doi.org/10.1007/bf02515826.

[12] A.I.K. Butt, M. Imran, S. Batool, M.A. Nuwairan, Theoretical Analysis of a COVID-19 CF-Fractional Model to Optimally Control the Spread of Pandemic, Symmetry. 15 (2023), 380. https://doi.org/10.3390/sym15020380.

[13] M. El-Shahed, A.M. Al-Dubiban, Mathematical Modelling of Lesser Date Moth Using Sex Pheromone Traps and Natural Enemies, Math. Probl. Eng. 2021 (2021), 8835321. https://doi.org/10.1155/2021/8835321.

[14] M. El-Shahed, A. Al-Nujiban, N.F. Abdel-Baky, Stochastic Modelling of Red Palm Weevil Using Chemical Injection and Pheromone Traps, Axioms. 11 (2022), 334. https://doi.org/10.3390/axioms11070334.

[15] Y. Alnafisah, M. El-Shahed, Optimal Control of Red Palm Weevil Model Incorporating Sterile Insect Technique, Mechanical Injection, and Pheromone Traps, Alexandria Eng. J. 93 (2024), 382–391. https://doi.org/10.1016/j.aej.2024.02.059.

[16] H. Barclay, P. van den Driessche, Pheromone Trapping Models for Insect Pest Control, Popul. Ecol. 25 (1983), 105–115. https://doi.org/10.1007/bf02528786.

[17] H.J. Barclay, J. Hendrichs, Models for Assessing the Male Annihilation ofBactroceraspp. with Methyl Eugenol Baits, Ann. Entomol. Soc. Amer. 107 (2014), 81–96. https://doi.org/10.1603/an13046.

[18] R. Anguelov, C. Dufourd, Y. Dumont, Mathematical Model for Pest–insect Control Using Mating Disruption and Trapping, Appl. Math. Model. 52 (2017), 437–457. https://doi.org/10.1016/j.apm.2017.07.060.

[19] J.P. Ntahomvukiye, A. Temgoua, S. Bowong, Study of the Population Dynamics of Busseola fusca, Maize Pest, Acta Biotheor. 66 (2018), 379–397. https://doi.org/10.1007/s10441-018-9335-x.

[20] S. Xiang, Y. Pei, X. Liang, Analysis and Optimization Based on a Sex Pheromone and Pesticide Pest Model With Gestation Delay, Int. J. Biomath. 12 (2019), 1950054. https://doi.org/10.1142/s1793524519500542.

[21] M.D. Tapi, L. Bagny-Beilhe, Y. Dumont, Miridae Control Using Sex-Pheromone Traps. Modeling, Analysis and Simulations, Nonlinear Anal.: Real World Appl. 54 (2020), 103082. https://doi.org/10.1016/j.nonrwa.2019.103082.

[22] M. El-shahed, A. M. Al-Dububan, Deterministic and Stochastic Fractional Order Model for Lesser Date Moth, Computer Syst. Sci. Eng. 40 (2022), 749–764. https://doi.org/10.32604/csse.2022.019655.

[23] G. Birkhoff, G. Rota, Ordinary Differential Equation, 4th Edition, Wily, New York, (1989).

[24] K. Hassan, A. Mustafa, M. Hama, An Eco-Epidemiological Model Incorporating Harvesting Factors, Symmetry. 13 (2021), 2179. https://doi.org/10.3390/sym13112179.

[25] W. Feng, N. Rocco, M. Freeze, X. Lu, Mathematical Analysis on an Extended Rosenzweig-Macarthur Model of Tri-Trophic Food Chain, Discrete Contin. Dyn. Syst. - S. 7 (2014). 1215–1230. https://doi.org/10.3934/dcdss.2014.7.1215.

[26] W. Feng, M. T. Cowen, X. Lu, Coexistence and Asymptotic Stability in Stage-Structured Predator-Prey Models, Math. Biosci. Eng. 11 (2014), 823–839. https://doi.org/10.3934/mbe.2014.11.823.

[27] P. van den Driessche, J. Watmough, Reproduction Numbers and Sub-Threshold Endemic Equilibria for Compartmental Models of Disease Transmission, Math. Biosci. 180 (2002), 29–48. https://doi.org/10.1016/s0025-5564(02)00108-6.

[28] A.J. Alqarni, A.S. Rambely, I. Hashim, Dynamic Modelling of Interactions Between Microglia and Endogenous Neural Stem Cells in the Brain During a Stroke, Mathematics. 8 (2020), 132. https://doi.org/10.3390/math8010132.

[29] K. Manna, V. Volpert, M. Banerjee, Dynamics of a Diffusive Two-Prey-One-Predator Model with Nonlocal Intra-Specific Competition for Both the Prey Species, Mathematics. 8 (2020), 101. https://doi.org/10.3390/math8010101.

[30] A.E. Matouk, A.A. Elsadany, E. Ahmed, H.N. Agiza, Dynamical Behavior of Fractional-Order Hastings–powell Food Chain Model and Its Discretization, Commun. Nonlinear Sci. Numer. Simul. 27 (2015), 153–167. https://doi.org/10.1016/j.cnsns.2015.03.004.

[31] L. Perko, Differential Equations and Dynamical Systems, Vol. 7, Texts in Applied Mathematics, Springer, 2013.

[32] L.S. Pontryagin, Mathematical Theory of Optimal Processes, CRC Press, 1987.

[33] J. Chowdhury, F. Al Basir, Y. Takeuchi, M. Ghosh, P.K. Roy, A Mathematical Model for Pest Management in Jatropha Curcas With Integrated Pesticides - An Optimal Control Approach, Ecol. Complex. 37 (2019), 24–31. https://doi.org/10.1016/j.ecocom.2018.12.004.

[34] E. Venturino, P.K. Roy, F. Al Basir, A. Datta, A Model for the Control of the Mosaic Virus Disease in Jatropha Curcas Plantations, Energ. Ecol. Environ. 1 (2016), 360–369. https://doi.org/10.1007/s40974-016-0033-8.

[35] H.T. Alemneh, A.S. Kassa, A.A. Godana, An Optimal Control Model With Cost Effectiveness Analysis of Maize Streak Virus Disease in Maize Plant, Infect. Dis. Model. 6 (2021), 169–182. https://doi.org/10.1016/j.idm.2020.12.001.

[36] N.H. Shah, P.M. Pandya, A.H. Suthar, Optimal Control to Curtail the Spread of COVID-19 Through Social Gatherings: A Mathematical Model, in: Mathematical and Computational Modelling of Covid-19 Transmission, River Publishers, pp. 109–124, 2023.